Numerical Comparison of Local Risk-Minimisation and Mean-Variance Hedging

David Heath,[1] Eckhard Platen[1] and Martin Schweizer[2]

Abstract: This paper provides comparative results on prices, hedging strategies and risks for local risk-minimisation and mean-variance hedging for a class of stochastic volatility models. A pricing and hedging framework is presented for both approaches with detailed analysis undertaken for the well-known Heston and Stein/Stein stochastic volatility models. These illustrate important quantitative differences between the two approaches.

2000 *Mathematics Subject Classification:* 62P05, 91B28, 60H30, 65U05, 65C05, 58G40.
JEL Classification: G10

Key words: incomplete markets, option pricing, hedging, local risk-minimisation, mean-variance hedging, stochastic volatility, PDE and simulation methods.

(in: E. Jouini, J. Cvitanić, M. Musiela (eds.), "Option Pricing, Interest Rates and Risk Management", Cambridge University Press (2001), 509–537)

This version: November 2002

[1]University of Technology Sydney, School of Finance & Economics and School of Mathematical Sciences, PO Box 123, Broadway, NSW, 2007, Australia
[2]Technische Universität Berlin, Fachbereich Mathematik, MA 7-4, Straße des 17. Juni 136, D - 10623 Berlin, Germany

1 Introduction

At present there is much uncertainty in the choice of the pricing measure for the hedging of derivatives in incomplete markets. Incompleteness can arise for instance in the presence of stochastic volatility, as will be studied in the following. This paper provides comparative numerical results for two important hedging methodologies, namely local risk-minimisation and global mean-variance hedging.

We first describe the theoretical framework that underpins these two approaches. Some comparative studies are then presented on expected squared total costs and the asymptotics of these costs, differences in prices and optimal hedge ratios. In addition, the density functions for squared total costs and proportional transaction costs are estimated as well as mean transaction costs as a function of hedging frequency. Numerical results are obtained for variations of the Heston and the Stein/Stein stochastic volatility models.

To produce accurate and reliable estimates, combinations of partial differential equation and simulation techniques have been developed that are of independent interest. Some explicit solutions for certain key quantities required for mean-variance hedging are also described. It turns out that mean-variance hedging is far more difficult to implement than what has been attempted so far for most stochastic volatility models. In particular the mean-variance pricing measure is in many cases difficult to identify and to characterise. Furthermore, the corresponding optimal hedge, due to its global optimality properties, no longer appears as a simple combination of partial derivatives with respect to state variables. It has more the character of an optimal control strategy.

The importance of this paper is that it documents for some typical stochastic volatility models some of the quantitative differences that arise for two major hedging approaches. We conclude by drawing attention to certain observations that have implications for the practical implementation of stochastic volatility models.

2 A Markovian Stochastic Volatility Framework

We consider a frictionless market in continuous time with a single primary asset available for trade. We denote by $S = \{S_t,\, 0 \leq t \leq T\}$ the price process for this asset defined on the filtered probability space $(\Omega, \mathcal{F}, P)$ with filtration $\mathbb{F} = (\mathcal{F}_t)_{0 \leq t \leq T}$ satisfying the usual conditions for some fixed but arbitrary time horizon $T \in (0, \infty)$.

We introduce the discounted price process $X = \{X_t = \frac{S_t}{B_t},\, 0 \leq t \leq T\}$, where $B = \{B_t,\, 0 \leq t \leq T\}$ represents the savings account that accumulates interest at the continuously compounding interest rate.

We consider a general two-factor stochastic volatility model defined by stochastic

differential equations (SDEs) of the form

$$\begin{aligned} dX_t &= X_t\,(\mu(t,Y_t)\,dt + Y_t\,dW_t^1) \\ dY_t &= a(t,Y_t)\,dt + b(t,Y_t)(\varrho\,dW_t^1 + \sqrt{1-\varrho^2}\,dW_t^2) \end{aligned} \tag{2.1}$$

for $0 \le t \le T$ with given deterministic initial values $X_0 \in (0,\infty)$ and $Y_0 \in (0,\infty)$. Here the function μ is a given appreciation rate. The volatility component Y evolves according to a separate SDE with drift function a, diffusion function b and constant correlation $\varrho \in [-1,1]$. W^1 and W^2 denote independent standard Wiener processes under P. The component Y allows for an additional source of randomness but is not available as a traded asset.

To ensure that this Markovian framework provides a viable asset price model we assume that appropriate conditions hold for the functions μ, a, b so that the system of SDEs (2.1) admits a unique strong continuous solution for the vector process (X,Y) with a strictly positive discounted price process X and a volatility process Y. We take the filtration $\mathbb{F}$ to be the P-augmentation of the natural filtration generated by W^1 and W^2.

In order to price and hedge derivatives in an arbitrage free manner we assume that there exists an equivalent local martingale measure (ELMM) Q. This is a probability measure Q with the same null sets as P and such that X is a local martingale under Q.

We denote by $\mathbb{P}$ the set of all ELMMs Q. Our financial market is characterised by the system (2.1) together with the filtration $\mathbb{F}$ and is called incomplete if $\mathbb{P}$ contains more than one element.

In this paper we are in principle interested in the hedging of European style contingent claims with an $\mathcal{F}_T$-measurable square integrable random payoff H based on the dynamics given by (2.1). A specific choice for H which we will use later on for our numerical examples is the European put option with payoff given by

$$H = h(X_T) = (K - X_T)^+. \tag{2.2}$$

The requirement of $\mathcal{F}_T$-measurability and square integrability for the payoff H allows for many types of path dependent contingent claims and possibly even dependence on the evolution of the volatility process Y.

Subject to certain restrictions on the functions $\mu,\ a,\ b$ and parameter ϱ we can ensure, via an application of the Girsanov transformation, that there is an ELMM Q.

The condition that X should be a local Q-martingale fixes the effect of the Girsanov transformation on W^1 but allows for different transformations on the independent W^2. Consequently if $|\varrho| < 1$ the set $\mathbb{P}$ contains more than one element and our financial market is therefore incomplete.

In order to price and hedge derivatives in this incomplete market setting we need to somehow fix the ELMM Q. Currently there is no general agreement on how to choose a specific ELMM Q and a number of alternatives are being considered in the literature.

In this paper we will consider two quadratic approaches to hedging in incomplete markets; these are local risk-minimisation and mean-variance hedging. For either of these two approaches we require hedging strategies of the form $\varphi = (\vartheta, \eta)$, where ϑ is a predictable X-integrable process and η is an adapted process such that the value process $V(\varphi) = \{V_t(\varphi),\, 0 \leq t \leq T\}$ with

$$V_t(\varphi) = \vartheta_t\, X_t + \eta_t \tag{2.3}$$

is right-continuous for $0 \leq t \leq T$. Using the hedging strategy $\varphi = (\vartheta, \eta)$ means that we form at time t a portfolio with ϑ_t units of the traded risky asset X_t and η_t units of the savings account.

The cost process $C(\varphi) = \{C_t(\varphi),\, 0 \leq t \leq T\}$ is then given by

$$C_t(\varphi) = V_t(\varphi) - \int_0^t \vartheta_s\, dX_s \tag{2.4}$$

for $0 \leq t \leq T$ and $\varphi = (\vartheta, \eta)$. A hedging strategy φ is self-financing if $C(\varphi)$ is P-a.s. constant over the time interval $[0, T]$ and φ is called mean self-financing if $C(\varphi)$ is a P-martingale.

3 Local Risk-Minimisation

Intuitively the goal of local risk-minimisation is to minimise the local risk defined as the conditional second moment of cost increments under the measure P at each time instant.

With local risk-minimisation we only consider hedging strategies which replicate the contingent claim H at time T; that is we only allow hedging strategies φ such that

$$V_T(\varphi) = H \qquad\qquad P - \text{a.s.} \tag{3.1}$$

Subject to certain technical conditions it can be shown that finding a locally risk-minimising strategy is equivalent to finding a decomposition of H in the form

$$H = H_0^{\mathrm{lr}} + \int_0^T \xi_s^{\mathrm{lr}}\, dX_s + L_T^{\mathrm{lr}}, \tag{3.2}$$

where H_0^{lr} is constant, ξ^{lr} is a predictable process satisfying suitable integrability properties and $L^{\mathrm{lr}} = \{L_t^{\mathrm{lr}},\, 0 \leq t \leq T\}$ is a square integrable P-martingale with $L_0^{\mathrm{lr}} = 0$ and such that the product process $L^{\mathrm{lr}} M$ is in addition a P-martingale,

where M is the martingale part of X. The representation (3.2) is usually referred to as the Föllmer-Schweizer decomposition of H, see Föllmer & Schweizer (1991).

The locally risk-minimising hedging strategy is then given by

$$\vartheta_t^{\mathrm{lr}} = \xi_t^{\mathrm{lr}} \tag{3.3}$$

and

$$\eta_t^{\mathrm{lr}} = V_t(\varphi^{\mathrm{lr}}) - \vartheta_t^{\mathrm{lr}} X_t, \tag{3.4}$$

where

$$V_t(\varphi^{\mathrm{lr}}) = C_t(\varphi^{\mathrm{lr}}) + \int_0^t \vartheta_s^{\mathrm{lr}}\, dX_s \tag{3.5}$$

with

$$C_t(\varphi^{\mathrm{lr}}) = H_0^{\mathrm{lr}} + L_t^{\mathrm{lr}} \tag{3.6}$$

for $0 \leq t \leq T$.

As is shown in Föllmer & Schweizer (1991) and Schweizer (1995) there exists a measure $\hat{P}$, the so-called minimal ELMM, such that

$$V_t(\varphi^{\mathrm{lr}}) = E_{\hat{P}}[H \,|\, \mathcal{F}_t] \tag{3.7}$$

for $0 \leq t \leq T$, where the conditional expectation in (3.7) is taken under $\hat{P}$. The measure $\hat{P}$ is identified, subject to certain integrability conditions, by the Radon-Nikodým derivative

$$\frac{d\hat{P}}{dP} = \hat{Z}_T, \tag{3.8}$$

where

$$\hat{Z}_t = \exp\left(-\frac{1}{2}\int_0^t \left(\frac{\mu(s,Y_s)}{Y_s}\right)^2 ds - \int_0^t \frac{\mu(s,Y_s)}{Y_s}\, dW_s^1\right) \tag{3.9}$$

for $0 \leq t \leq T$.

Assuming $\hat{Z}$ is a P-martingale, the Girsanov transformation can be used to show that the processes $\hat{W}^1$ and $\hat{W}^2$ defined by

$$\hat{W}_t^1 = W_t^1 + \int_0^t \frac{\mu(s,Y_s)}{Y_s}\, ds \tag{3.10}$$

and

$$\hat{W}_t^2 = W_t^2 \tag{3.11}$$

for $0 \leq t \leq T$ are independent Wiener processes under $\hat{P}$. Consequently, using $\hat{W}^1$ and $\hat{W}^2$, the system of stochastic differential equations (2.1) becomes

$$\begin{aligned} dX_t &= X_t\, Y_t\, d\hat{W}_t^1 \\ dY_t &= \left(a(t,Y_t) - \frac{\varrho}{Y_t}(b\,\mu)(t,Y_t)\right) dt \\ &\quad + b(t,Y_t)\left(\varrho\, d\hat{W}_t^1 + \sqrt{1-\varrho^2}\, d\hat{W}_t^2\right) \end{aligned} \tag{3.12}$$

for $0 \leq t \leq T$.

Taking contingent claims of the form $H = h(X_T)$ for some given function $h : [0, \infty) \to I\!R$ and using the Markov property we can rewrite (3.7) in the form

$$\begin{aligned} V_t(\varphi^{\mathrm{lr}}) &= E_{\hat{P}}[h(X_T) \,|\, \mathcal{F}_t] \\ &= v_{\hat{P}}(t, X_t, Y_t) \end{aligned} \tag{3.13}$$

for some function $v_{\hat{P}}(t, x, y)$ defined on $[0, T] \times (0, \infty) \times I\!R$. Subject to certain regularity conditions we can show that $v_{\hat{P}}$ is the solution to the partial differential equation (PDE)

$$\frac{\partial v_{\hat{P}}}{\partial t} + \left(a - \frac{\varrho\, b\, \mu}{y}\right) \frac{\partial v_{\hat{P}}}{\partial y} + \frac{1}{2}\left(x^2\, y^2\, \frac{\partial^2 v_{\hat{P}}}{\partial x^2} + b^2\, \frac{\partial^2 v_{\hat{P}}}{\partial y^2} + 2\, \varrho\, x\, y\, b\, \frac{\partial^2 v_{\hat{P}}}{\partial x\, \partial y}\right) = 0 \tag{3.14}$$

on $(0, T) \times (0, \infty) \times I\!R$ with boundary condition

$$v_{\hat{P}}(T, x, y) = h(x) \tag{3.15}$$

for $x \in (0, \infty)$, $y \in I\!R$. Solving this PDE yields the pricing function (3.13) for local risk-minimisation.

Now it follows by application of Itô's formula together with (3.14) that

$$V_t(\varphi^{\mathrm{lr}}) = V_0(\varphi^{\mathrm{lr}}) + \int_0^t \vartheta_s^{\mathrm{lr}}\, dX_s + L_t^{\mathrm{lr}}, \tag{3.16}$$

where

$$\vartheta_t^{\mathrm{lr}} = \frac{\partial v_{\hat{P}}}{\partial x}(t, X_t, Y_t) + \frac{\varrho}{X_t\, Y_t}\, b(t, Y_t) \frac{\partial v_{\hat{P}}}{\partial y}(t, X_t, Y_t) \tag{3.17}$$

and

$$L_t^{\mathrm{lr}} = \int_0^t \sqrt{1 - \varrho^2}\, b(s, Y_s) \frac{\partial v_{\hat{P}}}{\partial y}(s, X_s, Y_s)\, dW_s^2 \tag{3.18}$$

for $0 \leq t \leq T$.

Using (3.6) and (3.18) we see that the conditional expected squared cost on the interval $[t, T]$ for the locally risk-minimising strategy φ^{lr}, denoted by R_t^{lr}, is given by

$$\begin{aligned} R_t^{\mathrm{lr}} &= E\left[\left(C_T(\varphi^{\mathrm{lr}}) - C_t(\varphi^{\mathrm{lr}})\right)^2 \,\middle|\, \mathcal{F}_t\right] \\ &= E\left[\int_t^T (1 - \varrho^2) \left(b(s, Y_s) \frac{\partial v_{\hat{P}}}{\partial y}(s, X_s, Y_s)\right)^2 ds \,\middle|\, \mathcal{F}_t\right]. \end{aligned} \tag{3.19}$$

4 Mean-Variance Hedging

In this section we consider an alternative approach to hedging in incomplete markets based on what is called mean-variance hedging. Intuitively the goal here is to minimise the global quadratic risk over the entire time interval $[0, T]$. This contrasts with local risk-minimisation which focuses on minimisation of the second moments of infinitesimal cost increments.

With mean-variance hedging we allow strategies which do not fully replicate the contingent claim H at time T. However, we minimise

$$E\left[\left(H - V_0 - \int_0^T \vartheta_s \, dX_s\right)^2\right] \tag{4.1}$$

over an appropriate choice of initial value V_0 and hedge ratio ϑ. The pair of initial value and hedge ratio process which minimises this quantity is called the mean-variance optimal strategy and is denoted by $(V_0^{\mathrm{mvo}}, \vartheta^{\mathrm{mvo}})$ with

$$R_0^{\mathrm{mvo}} = E\left[\left(H - V_0^{\mathrm{mvo}} - \int_0^T \vartheta_s^{\mathrm{mvo}} \, dX_s\right)^2\right]. \tag{4.2}$$

Given an initial value V_0 and hedge ratio ϑ we can always construct a self-financing strategy $\varphi = (\vartheta, \eta)$ by choosing

$$\eta_t = V_0 + \int_0^t \vartheta_s \, dX_s - \vartheta_t \, X_t \tag{4.3}$$

for $0 \leq t \leq T$. The quantity

$$H - V_T(\varphi) = H - V_0 - \int_0^T \vartheta_s \, dX_s \tag{4.4}$$

appearing in (4.1) is then the net loss or shortfall at time T using the strategy φ with payment H. For a more precise specification of mean-variance hedging see Heath, Platen & Schweizer (2000).

Using (2.4), (3.1) and the first equation in (3.19) we see that

$$\begin{aligned} R_0^{\mathrm{lr}} &= E\left[\left(H - V_0(\varphi^{\mathrm{lr}}) - \int_0^T \vartheta_u^{\mathrm{lr}} \, dX_u\right)^2\right] \\ &\geq E\left[\left(H - V_0^{\mathrm{mvo}} - \int_0^T \vartheta_u^{\mathrm{mvo}} \, dX_u\right)^2\right] = R_0^{\mathrm{mvo}}. \end{aligned}$$

Thus, mean-variance hedging by definition delivers expected squared costs which are less than or equal to those obtained for the locally risk-minimising strategy.

Under suitable conditions it can be shown that the contingent claim H admits a decomposition of the form

$$H = \tilde{H}_0 + \int_0^T \tilde{\xi}_s \, dX_s + \tilde{L}_T, \tag{4.5}$$

where

$$V_0^{\mathrm{mvo}} = \tilde{H}_0 = E_{\tilde{P}}[H], \tag{4.6}$$

$\tilde{\xi}$ is a predictable process satisfying suitable integrability properties and $\tilde{L}$ is a $\tilde{P}$-martingale with $\tilde{L}_0 = 0$. The ELMM $\tilde{P}$ in (4.6) is the so-called variance-optimal measure; it appears naturally as the solution of a problem dual to minimising (4.1).

If we choose a self-financing strategy $\varphi^{\mathrm{mvo}} = (\vartheta^{\mathrm{mvo}}, \eta^{\mathrm{mvo}})$ with η^{mvo} defined as in (4.3) then using (4.5) and (4.6) the net loss at time T is given by

$$\begin{aligned} H - V_T(\varphi^{\mathrm{mvo}}) &= H - V_0^{\mathrm{mvo}} - \int_0^T \vartheta_s^{\mathrm{mvo}} \, dX_s \\ &= \tilde{L}_T + \int_0^T \left(\tilde{\xi}_s - \vartheta_s^{\mathrm{mvo}} \right) dX_s. \end{aligned} \tag{4.7}$$

Under suitable conditions and with $\varrho = 0$ it can be shown that $\tilde{P}$ can be identified from its Radon-Nikodým derivative in the form

$$\frac{d\tilde{P}}{dP} = \tilde{Z}_T, \tag{4.8}$$

where

$$\begin{aligned} \tilde{Z}_t &= \exp\left(- \int_0^t \frac{\mu(s, Y_s)}{Y_s} \, dW_s^1 - \int_0^t \tilde{\nu}_s \, dW_s^2 \right. \\ &\qquad \left. - \frac{1}{2} \int_0^t \left[\left(\frac{\mu(s, Y_s)}{Y_s} \right)^2 + (\tilde{\nu}_s)^2 \right] ds \right) \end{aligned} \tag{4.9}$$

with

$$\tilde{\nu}_t = b(t, Y_t) \, \frac{\partial J}{\partial y}(t, Y_t) \tag{4.10}$$

and

$$J(t, y) = - \log E \left[\exp\left(- \int_t^T \left(\frac{\mu(s, Y_s^{t,y})}{Y_s^{t,y}} \right)^2 ds \right) \right] \tag{4.11}$$

for $0 \leq t \leq T$. Here we denote by $Y^{t,y}$ the volatility process that starts at time t with value y and evolves according to the SDE (2.1).

Applying the Feynman-Kac formula to the function $\exp(-J)$ and using a transformation of variables back to the function J it can be shown that, under appropriate conditions for a, b and μ, J satisfies the PDE

$$\frac{\partial J}{\partial t} + a \, \frac{\partial J}{\partial y} + \frac{1}{2} \, b^2 \, \frac{\partial^2 J}{\partial y^2} - \frac{1}{2} \, b^2 \left(\frac{\partial J}{\partial y} \right)^2 + \left(\frac{\mu}{y} \right)^2 = 0 \tag{4.12}$$

on $(0,T)\times\mathbb{R}$ with boundary conditions

$$J(T,y)=0.$$

Assuming $\tilde{Z}$ is a P-martingale, an application of the Girsanov transformation shows that the processes $\tilde{W}^1$ and $\tilde{W}^2$ defined by

$$\tilde{W}_t^1 = W_t^1 + \int_0^t \frac{\mu(s,Y_s)}{Y_s}\,ds \tag{4.13}$$

and

$$\tilde{W}_t^2 = W_t^2 + \int_0^t \tilde{\nu}_s\,ds \tag{4.14}$$

for $0\le t\le T$ are independent Wiener processes under $\tilde{P}$. Hence with respect to $\tilde{W}^1$ and $\tilde{W}^2$ the system of stochastic differential equations (2.1) becomes

$$\begin{aligned} dX_t &= X_t\,Y_t\,d\tilde{W}_t^1 \\ dY_t &= \left[a(t,Y_t) - b^2(t,Y_t)\,\frac{\partial J}{\partial y}(t,Y_t)\right]dt \\ &\quad + b(t,Y_t)\,d\tilde{W}_t^2 \end{aligned} \tag{4.15}$$

for $0\le t\le T$. Note that we have assumed $\varrho=0$.

As in the case for local risk-minimisation we consider European contingent claims of the form $H=h(X_T)$. For this type of payoff and again using the Markov property and prescription (4.3) we can express by (4.5) and (4.6) the initial value $V_0(\varphi^{\mathrm{mvo}})$ in the form

$$V_0(\varphi^{\mathrm{mvo}}) = V_0^{\mathrm{mvo}} = E_{\tilde{P}}[H] = v_{\tilde{P}}(0,X_0,Y_0) \tag{4.16}$$

for some function $v_{\tilde{P}}(t,x,y)$ defined on $[0,T]\times(0,\infty)\times\mathbb{R}$ such that

$$v_{\tilde{P}}(t,X_t,Y_t) = E_{\tilde{P}}[H\,|\,\mathcal{F}_t]. \tag{4.17}$$

Subject to certain regularity conditions, it can be shown that $v_{\tilde{P}}$ is the solution of the PDE

$$\frac{\partial v_{\tilde{P}}}{\partial t} + \left[a - b^2\,\frac{\partial J}{\partial y}\right]\frac{\partial v_{\tilde{P}}}{\partial y} + \frac{1}{2}\,x^2\,y^2\,\frac{\partial^2 v_{\tilde{P}}}{\partial x^2} + \frac{1}{2}\,b^2\,\frac{\partial^2 v_{\tilde{P}}}{\partial y^2} = 0 \tag{4.18}$$

on $(0,T)\times(0,\infty)\times\mathbb{R}$ with boundary condition

$$v_{\tilde{P}}(T,x,y) = h(x) \tag{4.19}$$

for $x\in(0,\infty)$, $y\in\mathbb{R}$.

Similar to the case for local risk-minimisation we can apply the Itô formula combined with (4.15), (4.16) and (4.18) to obtain

$$v_{\tilde{P}}(t, X_t, Y_t) = V_0^{\text{mvo}} + \int_0^t \tilde{\xi}_s \, dX_s + \tilde{L}_t, \tag{4.20}$$

where

$$\tilde{\xi}_t = \frac{\partial v_{\tilde{P}}}{\partial x}(t, X_t, Y_t) \tag{4.21}$$

and

$$\tilde{L}_t = \int_0^t b(s, Y_s) \frac{\partial v_{\tilde{P}}}{\partial y}(s, X_s, Y_s) \, d\tilde{W}_s^2 \tag{4.22}$$

for $0 \leq t \leq T$.

Also, under suitable conditions, it can be shown that the expected squared cost over the interval $[0, T]$ is given by

$$R_0^{\text{mvo}} = E\left[\int_0^T e^{-J(s,Y_s)} \, b^2(s, Y_s) \left(\frac{\partial v_{\tilde{P}}}{\partial y}(s, X_s, Y_s)\right)^2 ds\right]. \tag{4.23}$$

Furthermore, the mean-variance optimal hedge ratio ϑ^{mvo} is given in feedback form by

$$\vartheta_t^{\text{mvo}} = \tilde{\xi}_t + \frac{\mu(t, Y_t)}{X_t \, Y_t^2} \left(v_{\tilde{P}}(t, X_t, Y_t) - \tilde{H}_0 - \int_0^t \vartheta_s^{\text{mvo}} \, dX_s\right). \tag{4.24}$$

Thus in the case of mean-variance hedging the optimal hedge ratio ϑ^{mvo} is in general not equal to $\tilde{\xi}$ which is the integrand appearing in the decomposition (4.5). This might not have been expected based on the results obtained for local risk-minimisation and is due to the fact that ϑ_t^{mvo} has more the character of an optimal control variable.

Finally, in the case where $\tilde{P} = \hat{P}$, so that $v_{\tilde{P}} = v_{\hat{P}}$, and, again subject to certain conditions, see Heath, Platen & Schweizer (2000), it can be shown that

$$R_0^{\text{mvo}} = E\left[\int_0^T e^{-J(s,Y_s)} \, (1 - \varrho^2) \, b^2(s, Y_s) \left(\frac{\partial v_{\hat{P}}}{\partial y}(s, X_s, Y_s)\right)^2 ds\right], \tag{4.25}$$

which is similar to (4.23) but includes the case $\varrho \neq 0$.

5 Some Specific Models

In this section we will consider the application of both local risk-minimisation and mean-variance hedging to four stochastic volatility models. The purpose of this study is to compare various quantities for the two hedging approaches and the given models. This will provide insight into qualitative and quantitative differences for the two quadratic hedging approaches.

Model	Volatility Dynamics Y	Appreciation Rate μ
S1	$dY_t = \delta\,(\beta - Y_t)\,dt + k\,dW_t^2$	$\mu(t, Y_t) = \Delta\, Y_t$
S2	as above	$\mu(t, Y_t) = \gamma\,(Y_t)^2$
H1	$d(Y_t)^2 = \kappa\,(\theta - (Y_t)^2)\,dt + \Sigma\, Y_t\,(\varrho\,dW_t^1 + \sqrt{1-\varrho^2}\,dW_t^2)$	$\mu(t, Y_t) = \Delta\, Y_t$
H2	$d(Y_t)^2 = \kappa\,(\theta - (Y_t)^2)\,dt + \Sigma\, Y_t\,dW_t^2$	$\mu(t, Y_t) = \gamma\,(Y_t)^2$

Table 1: Model specifications.

The models which we examine are based on the Stein & Stein (1991) and Heston (1993) type stochastic volatility models with two different specifications for the appreciation rate function μ.

The four models with their specifications are summarised in Table 1. Here S1 and S2 are the two Stein/Stein type models and H1 and H2 are the two Heston type models. We assume that the constants δ, β, k, κ, θ, Σ are non-negative, with Δ and γ real valued and $\varrho \in [-1, 1]$. Note that non-zero correlation is allowed only for the H1 model. For the H1 and H2 models an SDE for the volatility component Y can be obtained via Itô's formula as follows:

$$dY_t = \left(\frac{4\,\kappa\,(\theta - Y_t^2) - \Sigma^2}{8\,Y_t}\right) dt + \frac{\Sigma}{2}\left(\varrho\,dW_t^1 + \sqrt{1-\varrho^2}\,dW_t^2\right). \tag{5.1}$$

For the S1 and H1 models it can be shown, see Heath, Platen & Schweizer (2000), that $\tilde{P} = \hat{P}$ and that

$$J(t, y) = \Delta^2 (T - t) \tag{5.2}$$

for $(t, y) \in [0, T] \times I\!R$. By (3.19) and (4.25) this means that

$$\begin{aligned} R_0^{\mathrm{mvo}} &= E\left[\int_0^T e^{-\Delta^2 (T-s)}\,(1-\varrho^2)\,b^2(s, Y_s)\left(\frac{\partial v_{\tilde{P}}}{\partial y}(s, X_s, Y_s)\right)^2 ds\right] \\ &\geq e^{-\Delta^2 T}\,R_0^{\mathrm{lr}}. \end{aligned} \tag{5.3}$$

In addition it can be shown that the locally risk-minimising strategy is given by (3.17).

In the next section we compute the locally risk-minimising strategies for both the S1 and H1 models based on the formulae (3.12), (3.14), (3.17), (3.19). We note

that the derivations and technical details provided in the papers Heath, Platen & Schweizer (2000) and Schweizer (1991) do not fully cover the case of $\varrho \neq 0$ for the H1 model that have also been included for comparative purposes in our study. However, the numerical results obtained do not indicate any particular problems with this case.

For the S2 and H2 models it can be shown, see again Heath, Platen & Schweizer (2000), that both the locally risk-minimising and mean-variance optimal hedging strategies exist for the case of a European put option. Note that for mean-variance hedging existence of the optimal strategy is established only for a sufficiently small time horizon T. However, also in this case the numerical experiments have been successfully performed for long time scales without apparent difficulties, as will be seen in the next section.

For the S2 and H2 models we have from (4.11) and Table 1 the function

$$J(t,y) = -\log E\left[\exp\left(-\gamma^2 \int_t^T (Y_s^{t,y})^2\, ds\right)\right]. \tag{5.4}$$

Fortunately for both models this function can be computed explicitly, see again Heath, Platen & Schweizer (2000). In the case of the S2 model the J function in (5.4) is denoted by the symbol J_{S2} and has the form

$$J_{\mathrm{S2}}(t,y) = f_0(T-t) + f_1(T-t)\,\frac{y}{k} + f_2(T-t)\,\frac{y^2}{k^2}. \tag{5.5}$$

For the S2 model we have $a(t,y) = \delta(\beta - y)$ and $b(t,y) = k$. Using these specifications for the drift and diffusion coefficients and substituting (5.5) into (4.12) we can show that the functions f_0, f_1 and f_2 satisfy the ordinary differential equations (ODEs)

$$\begin{aligned}
\frac{d}{d\tau} f_0(\tau) + f_1(\tau)\left(\frac{1}{2} f_1(\tau) - \frac{\beta\,\delta}{k}\right) - f_2(\tau) &= 0,\\
\frac{d}{d\tau} f_1(\tau) + f_1(\tau)\,(\delta + 2\, f_2(\tau)) - \frac{2\beta\delta}{k}\, f_2(\tau) &= 0,\\
\frac{d}{d\tau} f_2(\tau) + 2\, f_2(\tau)\,(\delta + f_2(\tau)) - k^2\,\gamma^2 &= 0,
\end{aligned} \tag{5.6}$$

with boundary conditions

$$f_0(0) = f_1(0) = f_2(0) = 0. \tag{5.7}$$

These equations can be solved explicitly, yielding

$$\begin{aligned}
f_2(\tau) &= \frac{\lambda\,\gamma_1\,e^{-2\gamma_1\tau}}{\lambda+\gamma_1-\lambda\,e^{-2\gamma_1\tau}}-\lambda,\\
f_1(\tau) &= \frac{1}{1+2\,\lambda\,\psi(\tau)}\left((2\,D-D')\,e^{-2\gamma_1\tau}-2\,D\,e^{-2\gamma_1\tau}\right)+D',\\
f_0(\tau) &= \frac{1}{2}\,\log(1+2\,\lambda\,\psi(\tau))-\left(\lambda+\frac{\delta^2\,\beta^2}{2\,k^2}\,\left(\frac{\delta^2}{\gamma_1^2}-1\right)\right)\tau-\frac{2\,D^2\,\psi(\tau)}{1+2\,\lambda\,\psi(\tau)}\\
&\quad+\frac{\delta^2\,\beta}{k\,\gamma_1^2}\left(\frac{1}{1+2\,\lambda\,\psi(\tau)}\left(2\,D\,e^{-\gamma_1\tau}-\left(D-\frac{1}{2}\,D'\right)e^{-2\gamma_1\tau}\right)-\left(D+\frac{1}{2}\,D'\right)\right)
\end{aligned}$$

with constants

$$\gamma_1=\sqrt{2\,k^2\,\gamma^2+\delta^2},\lambda=\frac{\delta-\gamma_1}{2},D=\frac{\delta\,\beta}{2\,k}\left(1-\frac{\delta^2}{\gamma_1^2}\right),D'=\frac{\delta\,\beta}{k}\left(1-\frac{\delta}{\gamma_1}\right)$$

and function

$$\psi(\tau)=\frac{1-e^{-2\gamma_1\tau}}{2\,\gamma_1}.$$

Although the calculations are somewhat lengthy it can be verified by direct substitution that these analytic expressions are indeed the solution of (5.6) – (5.7). This was also confirmed for the models considered in the next section by solving (5.6) – (5.7) numerically and comparing these results with those obtained from the analytic solution. Furthermore, the ODE formulation can be used in situations where we replace one or more of the constant coefficients δ, β or k with time-dependent deterministic functions satisfying suitable regularity conditions.

The $\tilde{P}$ dynamics for the volatility component Y for the S2 model can now be obtained from (4.15) with the formula

$$\frac{\partial J_{\mathrm{S2}}}{\partial y}(t,y)=\frac{f_1(T-t)}{k}+\frac{2\,f_2(T-t)\,y}{k^2}. \tag{5.8}$$

For the H2 model the J function in (5.4), denoted by J_{H2}, is given by the expression

$$J_{\mathrm{H2}}(t,y)=g_0(T-t)+g_1(T-t)\,y^2. \tag{5.9}$$

Using the H2 model specifications $a(t,y)=\frac{4\kappa(\theta-y^2)-\Sigma^2}{8y}$ and $b(t,y)=\frac{\Sigma}{2}$ and substituting (5.9) into (4.12) we see that the functions g_0 and g_1 satisfy the ODEs

$$\begin{aligned}
\frac{d}{d\tau}\,g_0(\tau)-\kappa\,\theta\,g_1(\tau) &= 0,\\
\frac{d}{d\tau}\,g_1(\tau)+g_1(\tau)\left(\kappa+\frac{1}{2}\,\Sigma^2\,g_1(\tau)\right)-\gamma^2 &= 0
\end{aligned} \tag{5.10}$$

with boundary conditions

$$g_0(0) = g_1(0) = 0. \tag{5.11}$$

These equations can also be solved explicitly with

$$\begin{aligned} g_0(\tau) &= -\frac{2\kappa\theta}{\Sigma^2} \ln\left(\frac{2\,\Gamma\, e^{\frac{\Gamma+\kappa}{2}\tau}}{(\Gamma+\kappa)(e^{\Gamma\tau}-1)+2\,\Gamma}\right), \\ g_1(\tau) &= \frac{2\,\gamma^2\,(e^{\Gamma\tau}-1)}{(\Gamma+\kappa)(e^{\Gamma\tau}-1)+2\,\Gamma} \end{aligned}$$

and

$$\Gamma = \sqrt{2\,\gamma^2\,\Sigma^2+\kappa^2}.$$

It can be shown by direct substitution that these analytic expressions are the solutions of (5.10) – (5.11). Also these ODEs can under appropriate conditions be used in versions of the H2 model with time-dependent deterministic parameters.

The $\tilde{P}$ dynamics for the volatility component Y for the H2 model can now be obtained from (4.15) with

$$\frac{\partial J_{\mathrm{H2}}}{\partial y}(t,y) = 2\,g_2(T-t)\,y. \tag{5.12}$$

For a justification of the approach using PDEs which is applied in the next section to all four combinations of models, see Heath & Schweizer (2000).

6 Computation of Expected Squared Costs, Prices and Hedge Ratios

The purpose of this section is to compare actual numerical results for both hedging approaches for the models previously introduced. Emphasis will be placed on experiments which highlight differences in key quantities such as prices, expected squared total costs and hedge ratios. For the four models and two hedging frameworks extensive experimentation has been performed with different parameter sets. Only a small subset of these results can be presented in this paper. Nevertheless these results indicate some crucial differences between the two approaches that might be of more general interest. In total eight different hedging problems had to be solved with corresponding numerical tools developed. For all numerical experiments considered here the contingent claim was taken to be a European put, see (2.2). This ensures the payoff function h is bounded and avoids integrability problems.

To solve numerically the PDEs (3.14)–(3.15) and (4.18)–(4.19) we employed finite difference approximations based on the Crank-Nicolson scheme. Some experimentation was also performed using the fully implicit scheme. To handle the

two-dimensional structures appearing in (3.14) and (4.18) we used the method of fractional steps or operator splitting. For a discussion on these and related techniques, see Fletcher (1988), Sections 8.2 – 8.5, and Hoffman (1993), Chapters 11 and 14.

Fractional step methods are usually easier to implement in the case where there is no correlation in the diffusion terms, that is $\varrho = 0$, and thus the term in (3.14) corresponding to the cross-term partial derivative $\frac{\partial^2 v_{\hat{P}}}{\partial x \, \partial y}$ is zero. In the H1 model which allows for non-zero correlation we obtained an orthogonalised system of equations by introducing the transformation

$$Z_t = \ln(X_t) - \frac{\varrho}{\Sigma} Y_t^2 \tag{6.1}$$

for $0 \leq t \leq T$ and $\Sigma > 0$.

By Itô's formula, together with (3.12) and (5.1), the evolution of Z is governed by the SDE

$$dZ_t = \left[\left(\frac{\varrho \, \kappa}{\Sigma} - \frac{1}{2} \right) Y_t^2 + \varrho^2 \, \Delta \, Y_t - \frac{\varrho \, \kappa \, \theta}{\Sigma} \right] dt + Y_t \left[(1 - \varrho^2) \, d\hat{W}_t^1 - \varrho \sqrt{1 - \varrho^2} \, d\hat{W}_t^2 \right] \tag{6.2}$$

for $0 \leq t \leq T$. Using this transformation for a European put option with strike price K we obtain from the Kolmogorov backward equation a transformed function $u_{\hat{P}}$ defined on $[0, T] \times I\!R \times I\!R$ which is the solution of the PDE

$$\begin{aligned} \frac{\partial u_{\hat{P}}}{\partial t} + \left[\left(\frac{\varrho \, \kappa}{\Sigma} - \frac{1}{2} \right) y^2 + \varrho^2 \, \Delta \, y - \frac{\varrho \, \kappa \, \theta}{\Sigma} \right] \frac{\partial u_{\hat{P}}}{\partial z} \\ + \left(\frac{4 \, \kappa \, \beta - \Sigma^2}{8 \, y} - \frac{\kappa \, y}{2} - \frac{\varrho \, \Sigma \, \Delta}{2} \right) \frac{\partial u_{\hat{P}}}{\partial y} \\ + \frac{1}{2} \, y^2 \, (1 - \varrho^2) \, \frac{\partial^2 u_{\hat{P}}}{\partial z^2} + \frac{\Sigma^2}{8} \, \frac{\partial^2 u_{\hat{P}}}{\partial y^2} \;\; = \;\; 0 \end{aligned} \tag{6.3}$$

on $(0, T) \times I\!R \times I\!R$ with boundary condition

$$u_{\hat{P}}(T, z, y) = \left(K - \exp\left(z + \frac{\varrho \, y^2}{\Sigma} \right) \right)^+ . \tag{6.4}$$

In terms of the original pricing function $v_{\hat{P}}$ we have the relation

$$v_{\hat{P}}(t, x, y) = u_{\hat{P}}(t, \ln(x) - \frac{\varrho \, y^2}{\Sigma}, y). \tag{6.5}$$

As noted previously, for the H1 model we have $\tilde{P} = \hat{P}$ and the corresponding locally risk-minimising and mean-variance prices are the same.

For the numerical experiments described in this paper the following default values were used: For the Heston and Stein/Stein models $\kappa = 5.0$, $\theta = 0.04$, $\Sigma = 0.6$,

$\delta = 5.0$, $\beta = 0.2$ and $k = 0.3$. Models other than the H1 model have $\varrho = 0.0$ and for the appreciation rate μ from Table 1 we took $\Delta = 0.5$ and $\gamma = 2.5$. Other default parameters were $X_0 = 100.0$ and $Y_0 = 0.2$ as initial values for X and Y and strike $K = 100.0$ and time to maturity $T = 1.0$ for option parameters.

To compute the expected squared costs on the interval $[0, T]$ given by (3.19) and (4.23), respectively, we introduce the functions ζ^{lr} and ζ^{mvo} defined on $[0, T] \times (0, \infty) \times I\!R$ and given by

$$\zeta^{\mathrm{lr}}(t, x, y) = (1 - \varrho^2)\, b^2(t, y) \left(\frac{\partial v_{\hat{P}}}{\partial y}(t, x, y) \right)^2 \tag{6.6}$$

and

$$\zeta^{\mathrm{mvo}}(t, x, y) = (1 - \varrho^2)\, e^{-J(t,y)}\, b^2(t, y) \left(\frac{\partial v_{\tilde{P}}}{\partial y}(t, x, y) \right)^2 \tag{6.7}$$

for $(t, x, y) \in [0, T] \times (0, \infty) \times I\!R$.

By (3.19) and (6.6) it follows that

$$R_t^{\mathrm{lr}} = E\left[\int_t^T \zeta^{\mathrm{lr}}(s, X_s, Y_s)\, ds \,\middle|\, \mathcal{F}_t \right].$$

We can now apply the Kolmogorov backward equation together with (2.1) to show that there is a function r^{lr} defined on $[0, T] \times (0, \infty) \times I\!R$ such that

$$r^{\mathrm{lr}}(t, X_t, Y_t) = R_t^{\mathrm{lr}}$$

and r^{lr} is the solution to the PDE

$$\frac{\partial r^{\mathrm{lr}}}{\partial t} + x\,\mu\,\frac{\partial r^{\mathrm{lr}}}{\partial x} + a\,\frac{\partial r^{\mathrm{lr}}}{\partial y} + \frac{1}{2}\left(x^2\, y^2\, \frac{\partial^2 r^{\mathrm{lr}}}{\partial x^2} + b^2\, \frac{\partial^2 r^{\mathrm{lr}}}{\partial y^2} + 2\, x\, y\, b\, \varrho\, \frac{\partial^2 r^{\mathrm{lr}}}{\partial x\, \partial y} \right) + \zeta^{\mathrm{lr}} = 0 \tag{6.8}$$

on $(0, T) \times (0, \infty) \times I\!R$ with boundary condition

$$r^{\mathrm{lr}}(T, x, y) = 0 \tag{6.9}$$

for $(x, y) \in (0, \infty) \times I\!R$. If we set $R_t^{\mathrm{mvo}} := E\left[\int_t^T \zeta^{\mathrm{mvo}}(s, X_s, Y_s)\, ds \,\middle|\, \mathcal{F}_t \right]$ for $0 \leq t \leq T$ a completely analogous result holds for a function r^{mvo} with ζ^{mvo} replacing ζ^{lr} in (6.8).

Here we have used the system of equations (2.1) because for both hedging approaches the expected squared costs are computed under the real-world measure P. Note that for numerical solvers applied to (6.8) together with (6.9) the solutions to the pricing functions $v_{\hat{P}}$ and $v_{\tilde{P}}$ need to be pre-computed or at least made available at the current time step. For the H1 model with $\varrho \neq 0$ the transformed variable Z_t from (6.1) can be introduced to obtain orthogonalised equations for both hedging approaches, as has been explained for the pricing function $v_{\hat{P}}$.

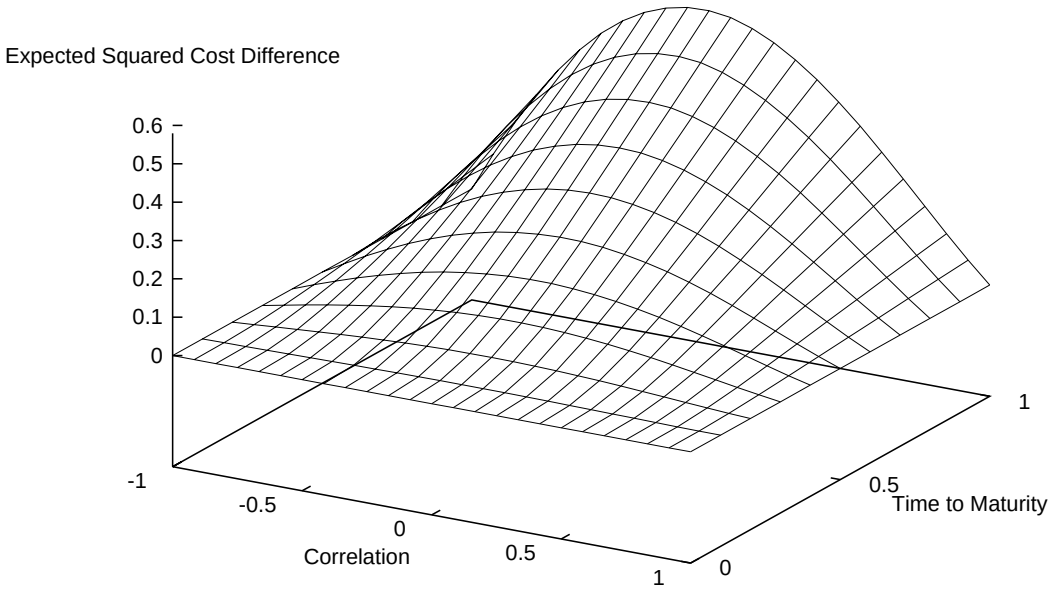

Figure 1: Expected squared cost differences ($R_0^{\mathrm{lr}} - R_0^{\mathrm{mvo}}$) for the H1 model.

To illustrate the difference in expected squared costs ($R_0^{\mathrm{lr}} - R_0^{\mathrm{mvo}}$) over the time interval $[0, T]$ we show in Figure 1 for the H1 model these differences using different values for the correlation parameter ϱ and time to maturity T. The absolute values of expected squared costs increase as T increases. For $T = 1.0$ and $\varrho = 0.0$ the computed values for prices and expected squared costs were $V_0(\varphi^{\mathrm{lr}}) = V_0(\varphi^{\mathrm{mvo}}) = 7.691$, $R_0^{\mathrm{lr}} = 4.257$ and $R_0^{\mathrm{mvo}} = 3.685$. For $T = 1.0$ and $\varrho = -0.5$ the computed values were $V_0(\varphi^{\mathrm{lr}}) = V_0(\varphi^{\mathrm{mvo}}) = 10.662$, $R_0^{\mathrm{lr}} = 4.429$ and $R_0^{\mathrm{mvo}} = 3.836$. Both R_0^{lr} and R_0^{mvo} tend to zero as $|\varrho|$ tends to 1, as can be expected from equations (3.19) and (4.24). This is also apparent from the fact that $|\varrho| = 1$ results in a complete market.

For increasing time to maturity T our numerical results indicate that R_0^{mvo} tends to zero. A similar remark has also been made by Hipp (1993). This observation is highlighted in Figure 2 which displays both R_0^{lr} and R_0^{mvo} over the time interval $[0, 100]$. In this sense the market can be considered as being "asymptotically complete" with respect to the mean-variance criterion. Similar results, which raise interesting questions concerning asymptotic completeness, are obtained for the other models H1, S2 and H2.

For the S2 and H2 models the drift specifications in Table 1 imply that $\hat{P} \neq \tilde{P}$ and consequently different prices are usually obtained for the two distinct measures and hedging strategies. Figure 3 illustrates these price differences for the model

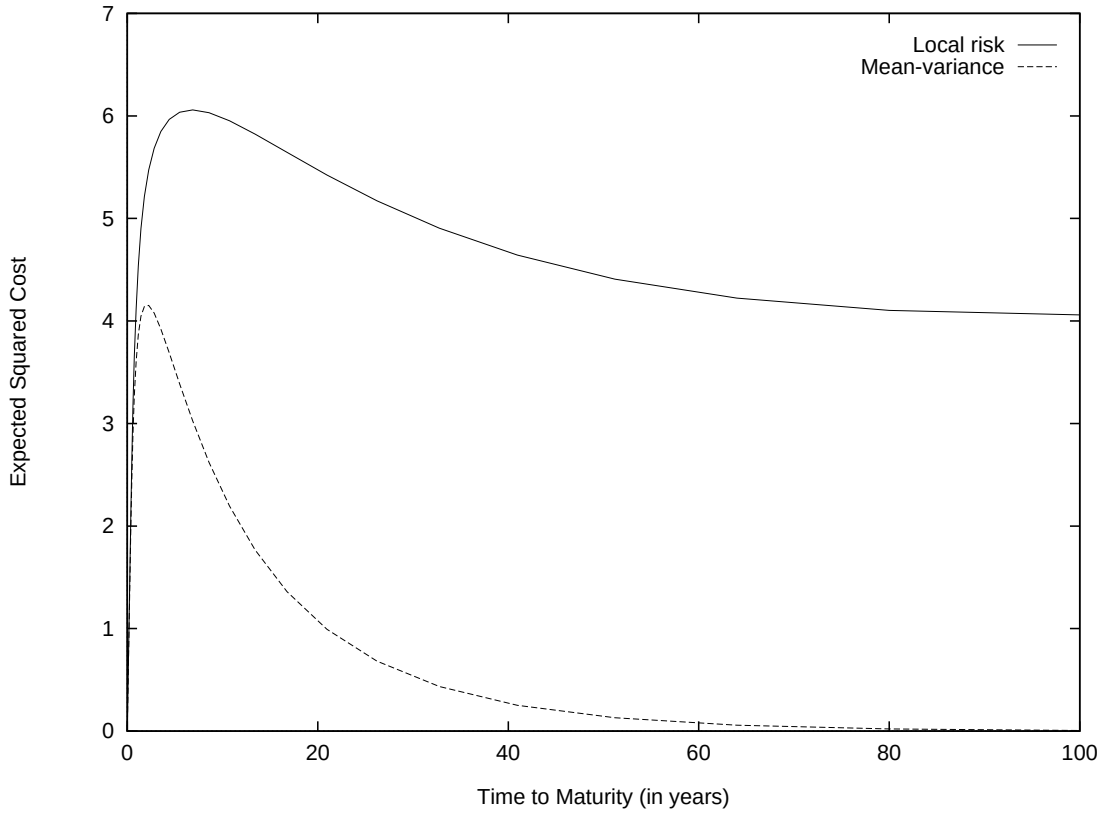

Figure 2: Expected squared costs R_0^{lr} and R_0^{mvo} over long time periods for the S1 model.

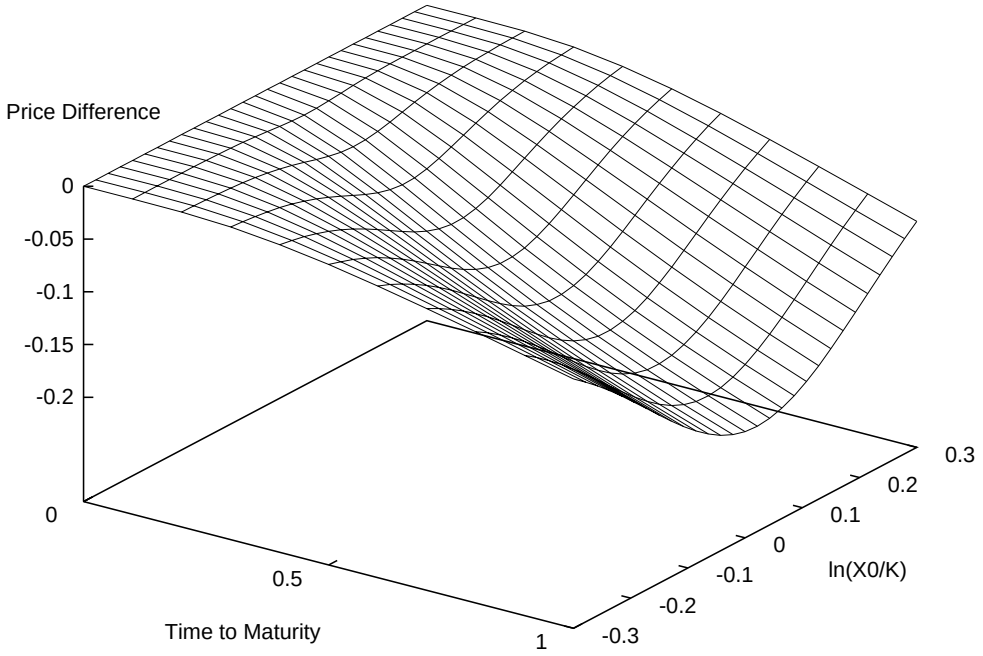

Figure 3: Price difference $(V_0(\varphi^{\mathrm{lr}}) - V_0(\varphi^{\mathrm{mvo}}))$ for the H2 model.

H2 using different values for time to maturity T and moneyness $\ln(\frac{X_0}{K})$.

For at-the-money options typical price differences of the order of 2–3% were obtained. For example, with input values $T = 1.0$ and $X_0 = K = 100.0$ the computed prices were $V_0(\varphi^{\mathrm{lr}}) = 7.6945$ and $V_0(\varphi^{\mathrm{mvo}}) = 7.892$. However, for an out-of-the money put option with $T = 1.0$ and $\ln(\frac{X_0}{K}) = 0.3$ greater relative price differences were obtained with output values $V_0(\varphi^{\mathrm{lr}}) = 0.764$ and $V_0(\varphi^{\mathrm{mvo}}) = 0.848$. For all data points computed, local risk-minimisation prices were lower than corresponding mean-variance prices, hence the differences shown in Figure 3 are negative. This means that for the parameter set and model considered here there is no obvious best candidate when choosing between the two hedging approaches. Mean-variance hedging delivers lower expected squared costs but it also results in what seem to be systematically different prices. Observe that put-call parity enforces lower prices for calls as opposed to higher prices for puts.

As is apparent from (5.3) the quantity $e^{-\Delta^2 T}$ provides a lower bound for the ratio $R_0^{\mathrm{mvo}}/R_0^{\mathrm{lr}}$ and the linear drift models H1 and S1. This bound is very good for small values of T; for example, with $T = 0.01$ the computed ratio and bound for the S1 model were $R_0^{\mathrm{mvo}}/R_0^{\mathrm{lr}} = 0.9982$ and $e^{-\Delta^2 T} = 0.9982$. With $T = 1.0$ the corresponding values were $R_0^{\mathrm{mvo}}/R_0^{\mathrm{lr}} = 0.8672$ and $e^{-\Delta^2 T} = 0.7788$.

We will now consider the computation of hedge ratios ϑ^{lr} and ϑ^{mvo} for the locally risk-minimising and mean-variance optimal hedging strategies given by (3.17) and

(4.24), respectively. Our aim will be to obtain approximate hedge ratios at equi-spaced discrete times $0 = t_0 < t_1 < \ldots < t_N = T$ with step size $t_i - t_{i-1} = \frac{T}{N}$ for $i \in \{1, \ldots, N\}$ using simulation techniques. Noting the form of (3.17) and (4.24) it is apparent that the price functions $v_{\hat{P}}$ and $v_{\tilde{P}}$ need to be pre-computed in order to calculate hedge ratios.

Once $v_{\hat{P}}$ and $v_{\tilde{P}}$ are determined, say on a discrete grid by a numerical solver, the partial derivatives appearing in (3.17) and (4.24) can be approximated using finite differences.

To simulate a given sample path for the vector (X, Y) under the measure P, an order 1.0 weak predictor-corrector numerical scheme, see Kloeden & Platen (1999), Section 15.5, was applied to the system of equations (2.1) to obtain a set of estimates $(\bar{X}_{t_i}, \bar{Y}_{t_i})$ for (X_{t_i}, Y_{t_i}) for $i \in \{0, \ldots, N\}$ with $\bar{X}_0 = X_0$ and $\bar{Y}_0 = Y_0$. From these a set of approximate values $\bar{\vartheta}^{\mathrm{lr}}_{t_i}$ for the hedge ratio $\vartheta^{\mathrm{lr}}_{t_i}$ and $\bar{\xi}_{t_i}$ for the integrand $\tilde{\xi}_{t_i}$, $i \in \{0, \ldots, N\}$ were obtained. One problem with this procedure is that the set of points $(t_i, \bar{X}_{t_i}, \bar{Y}_{t_i})$ for $i \in \{0, \ldots, N\}$ may not lie on the grid used to compute $v_{\hat{P}}$ and $v_{\tilde{P}}$. This difficulty can be overcome by the application of multi-dimensional interpolation methods. Note that all three measures P, $\hat{P}$ and $\tilde{P}$ are used with these calculations: P is needed to simulate paths for the vector (X, Y) and $\hat{P}$ and $\tilde{P}$ are used to approximate the pricing functions $v_{\hat{P}}$ and $v_{\tilde{P}}$, respectively.

The estimates $\bar{\vartheta}^{\mathrm{mvo}}_{t_i}$, $i \in \{0, \ldots, N\}$ for the mean-variance optimal hedge ratio can now be obtained from the Euler type approximation scheme, see (4.24),

$$\bar{\vartheta}^{\mathrm{mvo}}_{t_i} = \bar{\xi}_{t_i} + \frac{\mu(t_i, \bar{Y}_{t_i})}{\bar{X}_{t_i}\, \bar{Y}^2_{t_i}} \left(v_{\tilde{P}}(t_i, \bar{X}_{t_i}, \bar{Y}_{t_i}) - v_{\tilde{P}}(0, X_0, Y_0) - \sum_{j=0}^{i-1} \bar{\vartheta}^{\mathrm{mvo}}_{t_j} (\bar{X}_{t_{j+1}} - \bar{X}_{t_j}) \right) \tag{6.10}$$

for $i \in \{1, \ldots, N\}$. In the case of the S2 and H2 models we have $\hat{P} \neq \tilde{P}$. In general this means that $v_{\hat{P}} \neq v_{\tilde{P}}$ and $\frac{\partial v_{\hat{P}}}{\partial x} \neq \frac{\partial v_{\tilde{P}}}{\partial x}$ and consequently it follows from (3.17), (4.21) and (4.24) with $\varrho = 0$ that for the initial hedge ratios $\bar{\vartheta}^{\mathrm{lr}}_0 \neq \bar{\vartheta}^{\mathrm{mvo}}_0$. For models S1 and H1, since $v_{\hat{P}} = v_{\tilde{P}}$, we then get equal initial hedge ratios $\bar{\vartheta}^{\mathrm{lr}}_0 = \bar{\vartheta}^{\mathrm{mvo}}_0$. This equality does not in general hold for $t \in (0, T)$.

Figures 4 and 5 plot the linearly interpolated hedge ratios $\bar{\vartheta}^{\mathrm{lr}}_{t_i}$ and $\bar{\vartheta}^{\mathrm{mvo}}_{t_i}$, $i \in \{0, \ldots, N\}$, for a European put option for the S2 model. Figure 4 displays hedge ratios for a sample path ending in the money whereas Figure 5 shows hedge ratios for a different sample path ending out of the money. The trajectories for $X/100$ and Y for both sample paths are illustrated in Figure 6. Note that the mean-variance optimal hedge ratio takes values in the open interval $(0, -1)$ at maturity. This indicates that there is no full replication of the contingent claim.

In the case of the linear drift models S1 and H1 the factor $\frac{\mu(t_i, \bar{Y}_{t_i})}{\bar{X}_{t_i}\, \bar{Y}^2_{t_i}}$ appearing in (6.10) reduces to $\frac{\Delta}{\bar{X}_{t_i}\, \bar{Y}_{t_i}}$. This factor becomes $\frac{\gamma}{\bar{X}_{t_i}}$ for the quadratic drift models S2 and H2. For the given default parameter set the approximate volatility values $\bar{Y}_{t_i}$, $i \in \{0, \ldots, N\}$ can be quite small. Consequently for the linear drift models

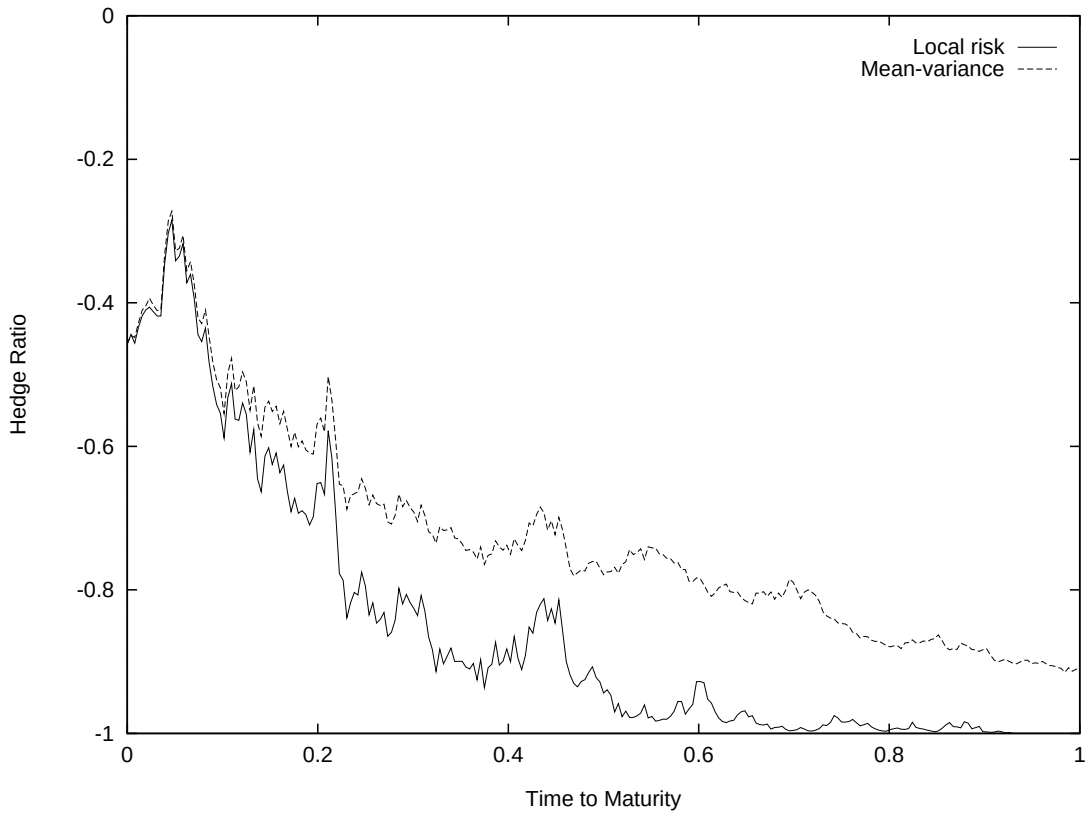

Figure 4: Hedge ratios for the S2 model: sample path ending in the money.

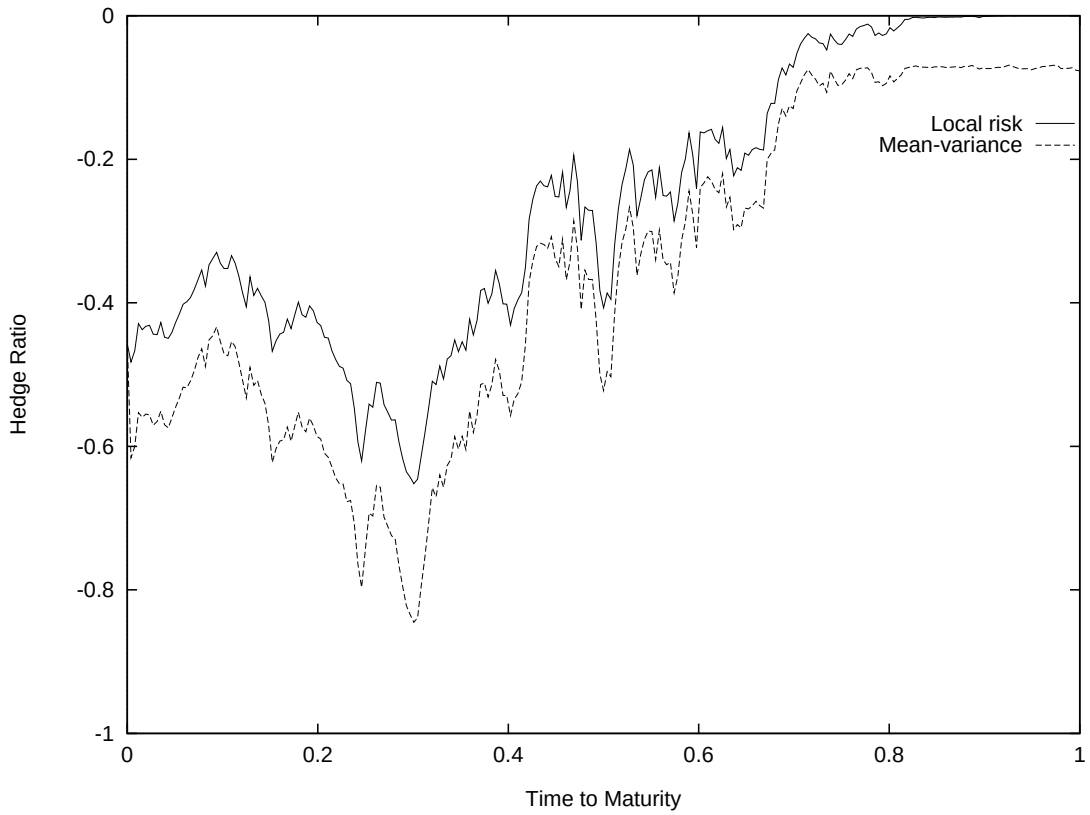

Figure 5: Hedge ratios for the S2 model: sample path ending out of the money.

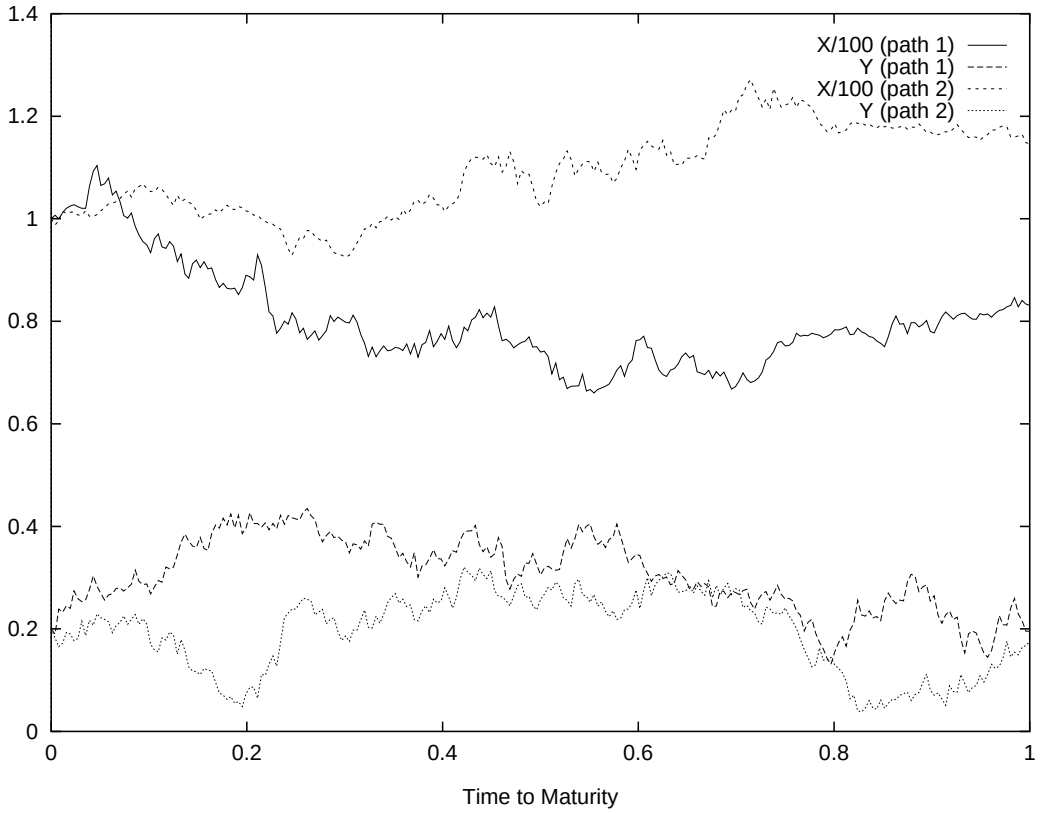

Figure 6: Two pairs of sample paths for the S2 model.

large fluctuations in the mean-variance optimal hedge ratios, compared to what is obtained under the locally risk-minimising criterion, can occur. Simulation experiments have shown that these differences are not so apparent for the quadratic drift models.

7 Distributions of Squared Costs

So far we have examined differences in expected squared costs for the two hedging approaches. It is also interesting to consider the distributions under the real-world measure P of the quantities

$$\varepsilon_t^{\mathrm{lr}} = \int_0^t \zeta^{\mathrm{lr}}(s, X_s, Y_s)\, ds \tag{7.1}$$

and

$$\varepsilon_t^{\mathrm{mvo}} = \int_0^t \zeta^{\mathrm{mvo}}(s, X_s, Y_s)\, ds \tag{7.2}$$

for $0 \leq t \leq T$, where ζ^{lr} and ζ^{mvo} are given by (6.6) and (6.7), respectively. In view of (3.17) and (4.24) these terms provide a measure for the squared costs on $[0, t]$ under local risk-minimisation and mean-variance hedging, respectively. To estimate the distributions of the random variables $\varepsilon_T^{\mathrm{lr}}$ and $\varepsilon_T^{\mathrm{mvo}}$ we used an order 1.0 weak predictor-corrector numerical scheme, see again Kloeden & Platen (1999), Section 15.5, to obtain a set of estimates $(\bar{X}_{t_i}, \bar{Y}_{t_i})$ for (X_{t_i}, Y_{t_i}) where, as in our hedging simulation experiments, $\{t_i;\, i \in \{0, \ldots, N\}\}$ is a set of increasing equi-spaced discrete times with $t_0 = 0$ and $t_N = T$. This enables us to compute a set of independent realisations of the random vector $(\bar{X}_{t_i}, \bar{Y}_{t_i})$ denoted by $(\bar{X}_{t_i}(\omega_j), \bar{Y}_{t_i}(\omega_j))$ for $i \in \{0, \ldots, N\}$ and $j \in \{1, \ldots, M\}$. From these, by applying a numerical integration routine using (7.1) and (7.2) we can generate a set of independent realisations $(\bar{\varepsilon}_T^{\mathrm{lr}}(\omega_j), \bar{\varepsilon}_T^{\mathrm{mvo}}(\omega_j))$ for the estimate $(\bar{\varepsilon}_T^{\mathrm{lr}}, \bar{\varepsilon}_T^{\mathrm{mvo}})$ of the squared costs.

We can also obtain sample path estimates of $(\varepsilon_T^{\mathrm{lr}}, \varepsilon_T^{\mathrm{mvo}})$ by using stochastic numerical methods applied to the full vector of components $(X, Y, \varepsilon^{\mathrm{lr}}, \varepsilon^{\mathrm{mvo}})$. Note that the approximation of the integrands ζ^{lr} and ζ^{mvo} appearing in (7.1) and (7.2) requires access to the solution of the pricing functions $v_{\hat{P}}$ and $v_{\tilde{P}}$. As was the case for the computation of hedge ratios, all three measures P, $\hat{P}$ and $\tilde{P}$ are involved in these calculations and multi-dimensional interpolation is needed to obtain values for $\zeta^{\mathrm{lr}}(t_i, \bar{X}_i, \bar{Y}_i)$ and $\zeta^{\mathrm{mvo}}(t_i, \bar{X}_i, \bar{Y}_i)$, $i \in \{0, \ldots, N\}$ along the paths of the simulated trajectories.

To obtain an estimate of the probability density function for the variates $\varepsilon_T^{\mathrm{lr}}$ and $\varepsilon_T^{\mathrm{mvo}}$ we use a histogram with K disjoint adjacent subintervals using the sample data $(\bar{\varepsilon}_T^{\mathrm{lr}}(\omega_j), \bar{\varepsilon}_T^{\mathrm{mvo}}(\omega_j))$ for $j \in \{1, \ldots, M\}$. The overall procedure can be enhanced by the inclusion of anti-thetic variates for both the X and Y components of our underlying diffusion process. Figure 7 shows the histogram of relative

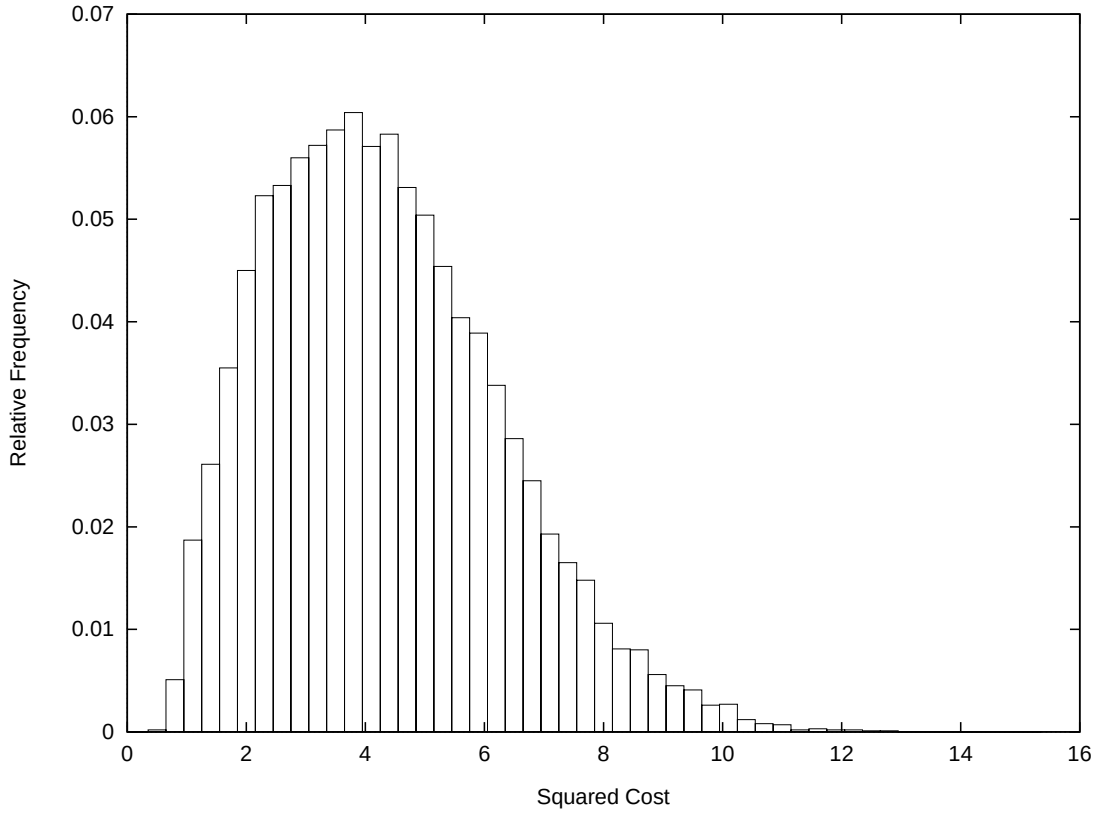

Figure 7: Squared cost histogram of $\varepsilon_T^{\mathrm{lr}}$ for the H1 model.

frequencies obtained for the squared costs $\varepsilon_T^{\mathrm{lr}}$ and the H1 model under the local risk-minimisation criterion with $N = 256$, $M = 16384$ and $K = 50$. Figure 8 shows the corresponding results for $\varepsilon_T^{\mathrm{mvo}}$. Histograms produced for the other three model combinations S1, H2 and S2 show a slightly more symmetric form for the density function. Similar results in a jump-diffusion model have been obtained by Grünewald & Trautmann (1997).

Of course the simulated data can be also used to compute the sample means

$$\frac{1}{M}\sum_{j=1}^{M}\bar{\varepsilon}_T^{\mathrm{lr}}(\omega_j) \quad \text{and} \quad \frac{1}{M}\sum_{j=1}^{M}\bar{\varepsilon}_T^{\mathrm{mvo}}(\omega_j)$$

for local risk-minimisation and mean-variance hedging, respectively. These provide estimates for the expected squared costs $R_0^{\mathrm{lr}} = E[\varepsilon_T^{\mathrm{lr}}]$ and $R_0^{\mathrm{mvo}} = E[\varepsilon_T^{\mathrm{mvo}}]$ which have been previously approximated via PDE methods, see (6.8) – (6.9). Consequently our Monte Carlo simulation can also be used to check our PDE results. A summary of these results using different values for $\ln(\frac{X_0}{K})$ with K fixed for the H1 model is given in Table 2.

The statistical errors reported in Table 2 were obtained at an approximate 99% confidence level. This was achieved by dividing the total number of outcomes into batches with sample means taken within each batch to form asymptotically

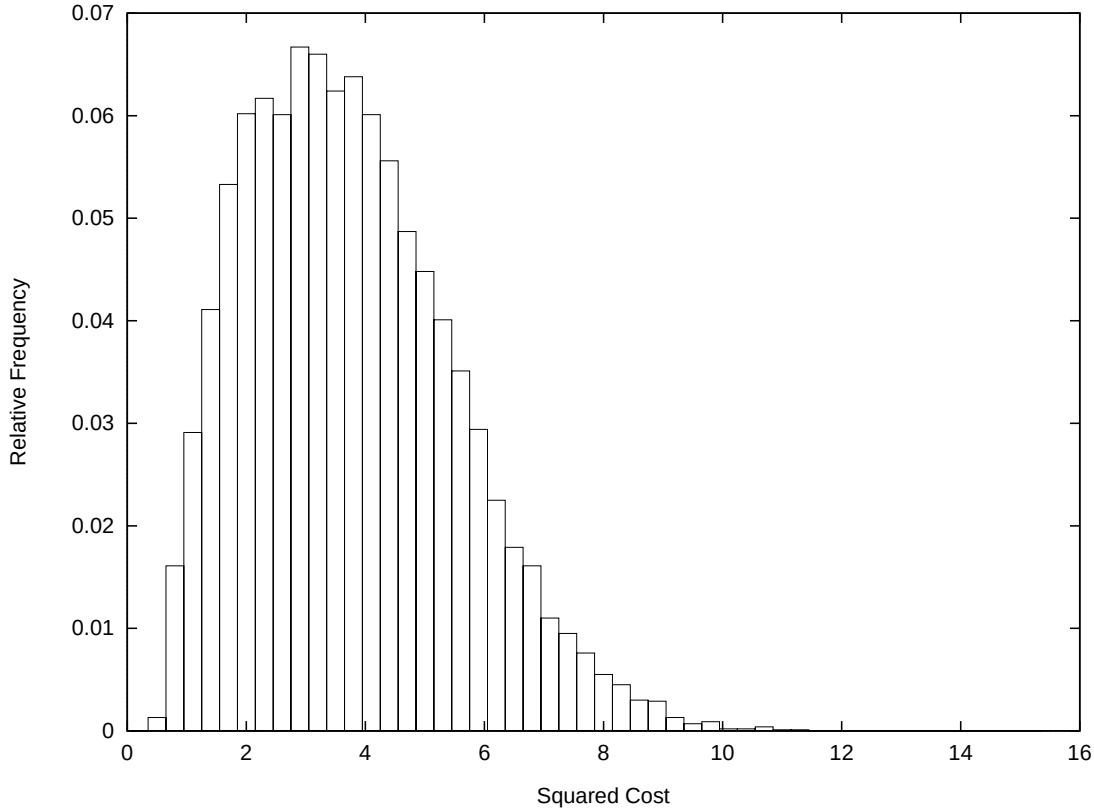

Figure 8: Squared cost histogram of $\varepsilon_T^{\text{mvo}}$ for the H1 model.

$\ln(X_0/K)$	PDE		Monte Carlo		Stat. error-99%	
	R_0^{lr}	R_0^{mvo}	R_0^{lr}	R_0^{mvo}	R_0^{lr}	R_0^{mvo}
0.3	0.775	0.672	0.789	0.685	0.023	0.020
0.2	1.812	1.566	1.836	1.587	0.027	0.024
0.1	3.294	2.843	3.310	2.856	0.026	0.024
0.0	4.257	3.685	4.273	3.697	0.074	0.066
-0.1	3.682	3.207	3.703	3.225	0.056	0.050
-0.2	2.278	2.003	2.293	2.016	0.025	0.022
-0.3	1.099	0.976	1.117	0.992	0.027	0.025

Table 2: Expected squared cost estimates using PDEs and Monte Carlo for the H1 model.

Gaussian statistics. It is apparent from Table 2 that both methodologies produce consistent results at least within the tolerance bounds computed for the Monte Carlo estimates. As an indication of the computing power required to produce these estimates, we mention that the expected squared costs obtained from PDE methods were computed in approximately 2 seconds (calculations performed on a Pentium MMX 233 MHz notebook). The Monte Carlo estimates using 16384 sample paths were computed in about 35 seconds.

8 Other Numerical Results

In Section 6 we considered the computation of approximate hedge ratios $\bar{\vartheta}^{\mathrm{lr}}$ and $\bar{\vartheta}^{\mathrm{mvo}}$ on a sample path by sample path basis. However, we would like to compare the variability of the competing hedge ratios using a more global criterion. One way of doing this is to assume proportional transaction costs.

A strategy ϑ applied at equi-spaced discrete transaction times $0 \leq t_0 < t_1 < \ldots < t_N = T$ would, in addition to the pure hedging costs, incur transaction expenses

$$\lambda\, S_N(\vartheta)$$

for some $\lambda > 0$, where $S_N(\vartheta)$ is given by

$$S_N(\vartheta) = \sum_{i=1}^{N} |\vartheta_{t_i} - \vartheta_{t_{i-1}}|\, X_{t_i}.$$

Since ϑ will typically be of infinite variation, we expect $S_N(\vartheta)$ to diverge as $N \to +\infty$. Consequently direct comparison of $S_N(\vartheta^{\mathrm{lr}})$ and $S_N(\vartheta^{\mathrm{mvo}})$ is difficult as both quantities become unbounded as N becomes large. However, the transaction cost ratio

$$r_N(\vartheta^{\mathrm{lr}}, \vartheta^{\mathrm{mvo}}) = \frac{S_N(\vartheta^{\mathrm{lr}})}{S_N(\vartheta^{\mathrm{mvo}})}$$

can be examined and compared, at least on the basis of simulation experiments. To do this we fix N and generate approximate hedge ratios $(\bar{\vartheta}^{\mathrm{lr}}_{t_i}, \bar{\vartheta}^{\mathrm{mvo}}_{t_i})$, for $i \in \{0, \ldots, N\}$, using the simulation methods outlined previously. These computations are performed with respect to the real-world measure P. The simulation data obtained enables us to determine $r_N(\bar{\vartheta}^{\mathrm{lr}}, \bar{\vartheta}^{\mathrm{mvo}})$ for a number of different sample paths and therefore to examine numerically the distributional properties of the estimate $r_N(\bar{\vartheta}^{\mathrm{lr}}, \bar{\vartheta}^{\mathrm{mvo}})$.

Figure 9 shows a histogram of relative frequencies for $\log_{10}(r_N(\bar{\vartheta}^{\mathrm{lr}}, \bar{\vartheta}^{\mathrm{mvo}}))$ and the S1 model formed with $N = 250$ transaction times and $M = 16384$ sample paths. As for our squared cost estimates, we used anti-thetic variates for each of the X and Y components in our underlying diffusion process. The value $N = 250$ corresponds approximately to daily hedging for the default time to maturity $T = 1$. Note that

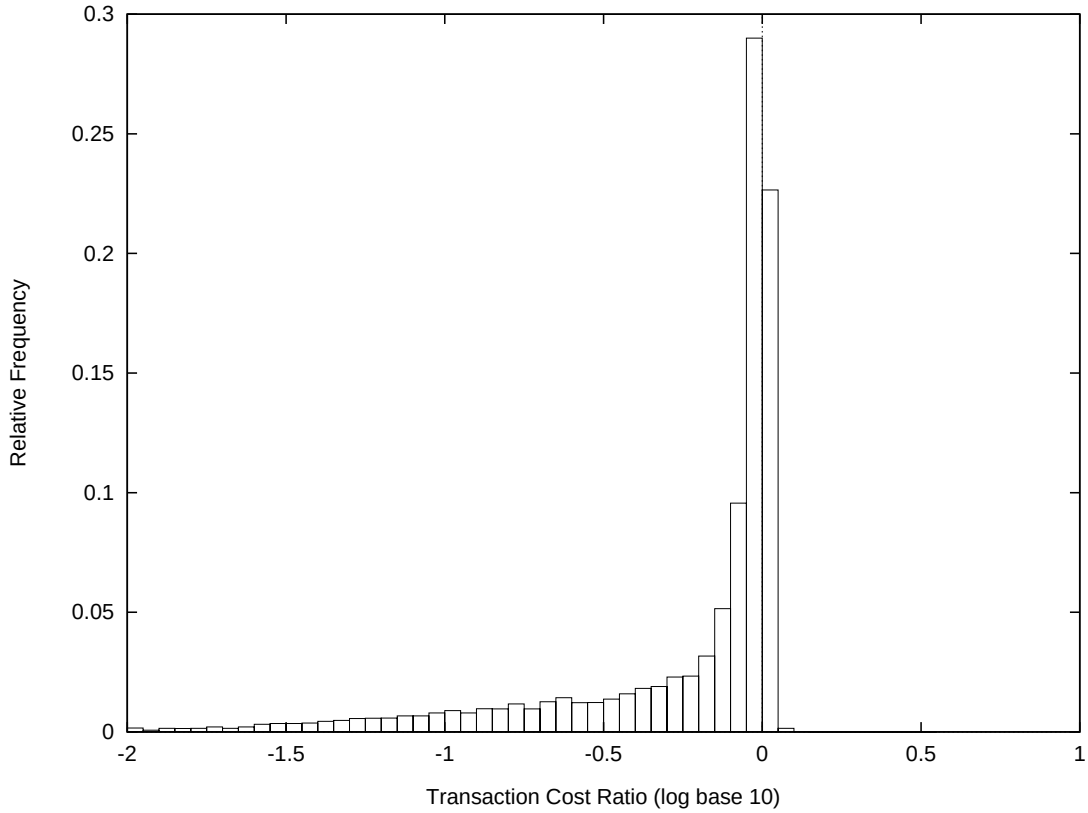

Figure 9: Transaction cost ratio histogram of $\log_{10}(r_N(\bar{\vartheta}^{\mathrm{lr}}, \bar{\vartheta}^{\mathrm{mvo}}))$ for the S1 model.

relative frequencies for the variable $\log_{10}(r_N(\bar{\vartheta}^{\mathrm{lr}}, \bar{\vartheta}^{\mathrm{mvo}}))$ rather than $r_N(\bar{\vartheta}^{\mathrm{lr}}, \bar{\vartheta}^{\mathrm{mvo}})$ are used. This is introduced to rescale the output so that it can be conveniently displayed in the form illustrated in Figure 9.

Figure 10 shows the corresponding histogram of relative frequencies for $\log_{10}(r_N(\bar{\vartheta}^{\mathrm{lr}}, \bar{\vartheta}^{\mathrm{mvo}}))$ using the H2 model and the same transaction times and sample paths. Note that the variability of transaction cost ratios in this model is much smaller than in the first one. In Figure 9 the range of values for $\log_{10}(r_N(\bar{\vartheta}^{\mathrm{lr}}, \bar{\vartheta}^{\mathrm{mvo}}))$ varies from -2 to 1 whereas in Figure 10 the range is from -0.15 to 0.15. Experimentation with the other model combinations H1 and S2 produced results which are similar to those obtained for S1 and H2 models, respectively. These results demonstrate that the distributional properties of $r_N(\vartheta^{\mathrm{lr}}, \vartheta^{\mathrm{mvo}})$ are highly dependent on our choice of the appreciation rate μ.

Experimentation with different choices of N does not seem to change these results dramatically. For example we can compute the sample mean $A(\bar{r}_N)$ of transaction cost ratios using the formula

$$A(\bar{r}_N) = \frac{1}{M} \sum_{i=1}^{M} \frac{S_N(\bar{\vartheta}^{\mathrm{lr}}(\omega_j))}{S_N(\bar{\vartheta}^{\mathrm{mvo}}(\omega_j))}.$$

Figure 11 shows the result of plotting $A(\bar{r}_N)$ for the S1, H1 and H2 models. The

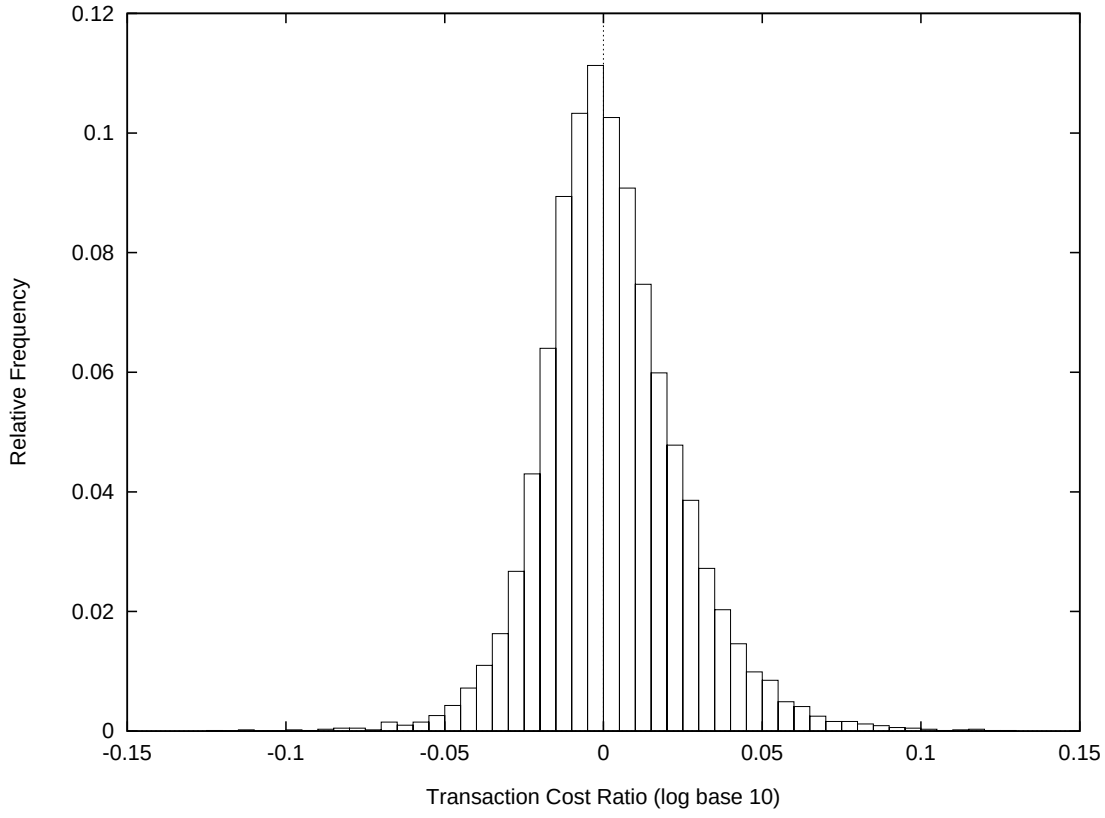

Figure 10: Transaction cost ratio histogram of $\log_{10}(r_N(\bar{\vartheta}^{\mathrm{lr}}, \bar{\vartheta}^{\mathrm{mvo}}))$ for the H2 model.

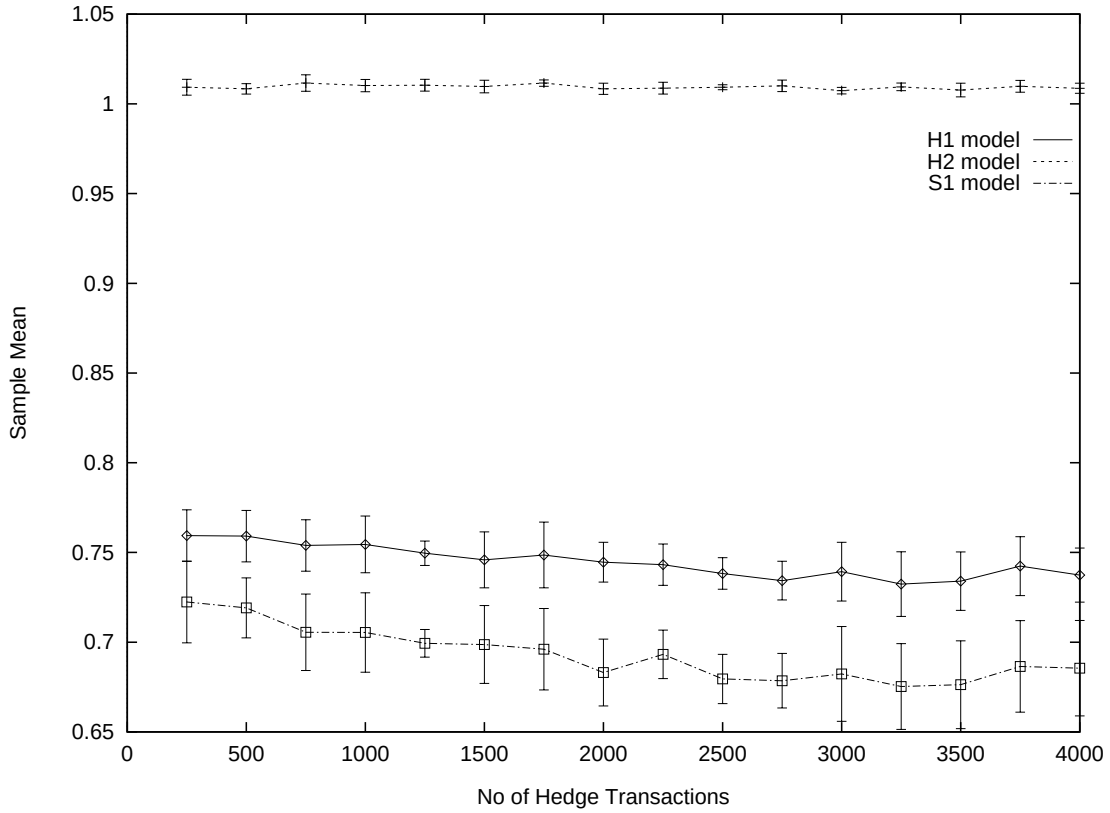

Figure 11: Sample means and confidence intervals for $A(\bar{r}_N)$.

error-bars displayed indicate approximate confidence intervals at a 99% level. The values for the S2 model are omitted because these are very close to those for the H2 model. The value $N = 4000$ would correspond to half-hourly hedging with an eight hour trading day and 250 trading days per year.

9 Conclusion

This paper documents some of the differences between local risk-minimisation and mean-variance hedging for some specific stochastic volatility models. We have shown that reliable and accurate estimates for prices, hedge ratios, total expected squared costs and other quantities can be obtained for both hedging approaches. Over long time periods it seems that the mean-variance criterion leads to a form of asymptotic completeness which is not the case for local risk-minimisation. For the quadratic drift models S2 and H2 mean-variance hedging delivers lower expected squared costs and seems to change prices in a systematic way.

Relative frequency histograms of squared costs show forms which are similar for both hedging approaches, with relative frequencies for mean-variance hedging having, in general, a more compressed shape compared to those for local risk-minimisa-

tion.

However, relative frequency histograms for transaction cost ratios show highly variable patterns which seem to depend mainly on the choice of the appreciation rate and which do not change significantly as the hedging frequency is increased.

Some of the results described in this paper raise a number of interesting theoretical and practical issues for future research such as the assessment of long term performance and extension of the numerical methods outlined in this paper to include more general specifications for the appreciation rate.

Acknowledgements

The authors gratefully acknowledge support by the School of Mathematical Sciences and the Faculty of Economics and Commerce of the Australian National University, the Schools of Mathematical Sciences and Finance and Economics of the University of Technology Sydney, the Fachbereich Mathematik of the Technical University of Berlin and the Deutsche Forschungsgemeinschaft.

References

Fletcher, C. A. J. (1988). *Computational Techniques for Fluid Dynamics* (2nd ed.), Volume 1 of *Springer Ser. Comput. Phys.* Springer.

Föllmer, H. & M. Schweizer (1991). Hedging of contingent claims under incomplete information. In M. Davis and R. Elliott (Eds.), *Applied Stochastic Analysis*, Volume 5 of *Stochastics Monogr.*, pp. 389–414. Gordon and Breach, London/New York.

Grünewald, B. & S. Trautmann (1997). Varianzminimierende Hedgingstrategien für Optionen bei möglichen Kurssprüngen. *Bewertung und Einsatz von Finanzderivaten, Zeitschrift für betriebswirtschaftliche Forschung* **38**, 43–87.

Heath, D., E. Platen, & M. Schweizer (2000). A comparison of two quadratic approaches to hedging in incomplete markets. *To appear in Mathematical Finance.*

Heath, D. & M. Schweizer (2000). Martingales versus PDEs in finance: An equivalence result with examples. *To appear in Journal of Applied Probability.*

Heston, S. L. (1993). A closed-form solution for options with stochastic volatility with applications to bond and currency options. *Rev. Financial Studies* **6**(2), 327–343.

Hipp, C. (1993). Hedging general claims. In *Proceedings of the 3rd AFIR Colloquium, Rome*, Volume 2, pp. 603–613.

Hoffman, J. D. (1993). *Numerical Methods for Engineers and Scientists.* McGraw-Hill, Inc.

Kloeden, P. E. & E. Platen (1999). *Numerical Solution of Stochastic Differential Equations*, Volume 23 of *Appl. Math.* Springer.

Schweizer, M. (1991). Option hedging for semimartingales. *Stochastic Process. Appl.* **37**, 339–363.

Schweizer, M. (1995). On the minimal martingale measure and the Föllmer-Schweizer decomposition. *Stochastic Anal. Appl.* **13**, 573–599.

Stein, E. M. & J. C. Stein (1991). Stock price distributions with stochastic volatility: An analytic approach. *Rev. Financial Studies* **4**, 727–752.